2796

Methods for Numerical Simulation of Water and Gas Coning

R. C. MacDONALD
JUNIOR MEMBER AIME
K. H. COATS*
MEMBER AIME

TEXAS PETROLEUM RESEARCH COMMITTEE
AUSTIN, TEX.
THE U. OF TEXAS
AUSTIN, TEX.

ABSTRACT

This paper describes and evaluates three numerical methods for the simulation of well coning behavior. The first method employs the implicit pressure-explicit saturation (IMPES) analysis with the production terms treated implicitly. The second technique is similar to the first model except that the interblock transmissibilities are also treated implicitly in the saturation equation. The third model is fully implicit with respect to all variables in a manner qualified in the Introduction and utilizes simultaneous solution of the difference equations describing the multiphase flow.

The use of implicit transmissibilities in the IMPES model results in a several-fold increase in the allowable time-increment size over that attainable with the implicit production IMPES scheme, while the computing time per step is increased by less than 10 percent. The fully implicit model accepts larger time-increment sizes than possible with the first two methods but requires 3.3 times the computing time per time step needed by the second model. The fully implicit model is substantially more efficient for problems involving high capillary forces (treated explicitly in the IMPES methods) and small computing grid blocks at the wellbore. In problems involving moderate capillary forces and larger grid spacings, the fully implicit method and the implicit transmissibility IMPES technique are comparable in computing efficiency. The results of three coning studies are presented: a water-oil problem, a three-phase coning example, and a comparison of simulation results with a laboratory coning experiment. Also presented is an analysis of truncation error and a comparison of computational work requirements.

Original manuscript received in Society of Petroleum Engineers office Jan. 20, 1970. Revised manuscript received July 15, 1970. Paper (SPE 2796) was presented at Second Symposium on Numerical Simulation of Reservoir Performance, held in Dallas, Tex., Feb. 5-6, 1970.

[1]References given at end of paper.

*Presently with International Computer Applications Ltd., Houston, Tex.

This paper will be printed in Transactions volume 249, which which will cover 1970.

INTRODUCTION

This study was performed to evaluate three finite-difference schemes for simulating well coning behavior. The basis for this evaluation was the IMPES (implicit pressure-explicit saturation) model with explicit transmissibilities and implicit production terms. This model is referred to hereafter as Model 1. The next model evaluated in this work is an IMPES model similar to Model 1, except that the saturation-dependent interblock transmissibilities are treated implicitly rather than explicitly in the saturation equation. The third model is fully implicit with respect to all variables and terms — transmissibilities, pressure, saturation and capillary pressure — and utilizes simultaneous solution of the difference equations describing the multiphase flow. These two models are referred to hereafter simply as Model 2 and Model 3. For the purpose of clarity all models are described in reference to the problem of incompressible, two-phase flow. The techniques are equally applicable, however, to compressible, three-phase flow models. The examples chosen for illustration employ both incompressible and compressible simulation models.

Fig. 1 illustrates the two-dimensional, cylindrical (r-z) system, extending from well radius r_w to

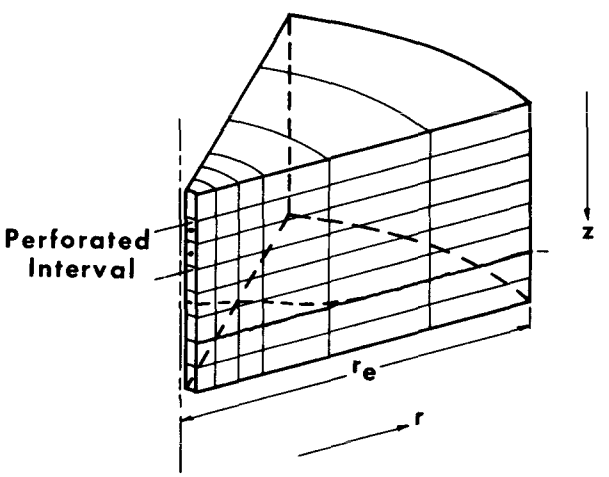

FIG. 1 — DIFFERENCE MODEL GRID SYSTEM.

exterior radius r_e. Arbitrary boundary conditions can easily be handled in the difference schemes described, including no-flow, specified flow or specified pressure. In this paper we use the no-flow boundary condition with edge influx or injection and production handled by source and sink terms in the blocks adjacent to the boundaries.

The term "fully implicit", used here in regard to Model 3 refers to the implicit treatment (dating at the new time level, $n+1$) of (a) pressures and capillary pressures and (b) saturations which appear as arguments in the transmissibilities and production rate terms. However, the pressure which also appears as an argument in the transmissibility and production rate terms is treated explicitly at time level n. We have found insignificant enhancement of model stability and accuracy to follow from implicit treatment of this pressure argument. In addition, in the "fully implicit" Model 3, a nonlinear term is dropped as described below in Eq. 30. Whether transmissibilities or production rate terms are involved, the use of the term "implicit" or "fully implicit" here refers to the dating of the saturation argument implicitly and the pressure argument explicitly.

Subsequent sections describe (1) the computational difficulties inherent in simulation of coning, (2) the general features of the difference schemes employed in the models, (3) the comparative results in efficiency (compute time per time step) and capability (maximum tolerable time step) including three example applications and (4) mathematical descriptions of the models. A more detailed description of Model 3 together with actual applications will be given in a subsequent paper.

THE CONING PROBLEM

Coning models are particularly subject to instability because of the convergent nature of the flow pattern. The pore volumes of the individual grid blocks typically decrease sharply near the wellbore, in part due to the cylindrical geometry and in part due to the use of small radial grid spacing near the wellbore. For reasonably sized time increments, the pore volume throughput (i.e., the flow through a grid block per pore volume of that block) in one of these smaller blocks near the wellbore is many times the pore volume of the block. During and after the breakthrough of the displacing phase, the relative amounts of each phase flowing into and out of a block are determined by the saturations in that and the adjacent grid blocks. These saturations are known only for the beginning of the time interval. If the relative flow of one phase into a block increases sharply, the use of the out-of-date saturation to compute the relative flow out of the block will result in the calculation of an unrealistically high value for the updated saturation. When the computations are continued to the next time step, just the opposite happens, and a low saturation value is found. The oscillation in saturation will continue in subsequent calculations, yielding meaningless results.

Control or elimination of this oscillation requires use of a sufficiently small time step which in turn results in high computing time and cost. A mathematical stability analysis shows that the restriction on time-step size results from treating such terms as transmissibilities, capillary pressure, and production terms explicitly rather than implicitly. Blair and Weinaug[1] showed that the restriction on time-step size necessary for computational stability can be eased by handling these terms implicitly. However, as a general rule, the required computing time per time step increases significantly as these various terms are treated implicitly rather than explicitly. Since we have for a given problem

$$\text{computing cost} = (\text{machine cost, \$/sec}) \times (\text{machine time, sec/time step}) (\text{number of time steps}),$$

we find that one cost factor rises and the other decreases as greater degrees of implicitness are incorporated in the difference scheme. The obvious question then in relation to difference schemes of increasing implicitness is whether the maximum tolerable time-step size continues to rise more than proportionately to the machine computing time per time step. Equivalently, we wish to find that method which minimizes the ratio of machine computing time per time step to tolerable time-step size.

Two factors detract somewhat from the quantitative simplicity of the above question. First, the programming labor increases considerably for methods of increasing degrees of implicitness. Second, computational stability is not the only factor limiting time-step size. Even an unconditionally stable difference scheme is subject to oscillation and/or inaccuracy when a sufficiently large time step is used, due to the presence of truncation error.

GENERAL DESCRIPTION OF THREE CONING MODELS

In this section we give a verbal description of each of the three models used in this study. A mathematical description of the first two models is presented later in the present paper, while the detailed description of the third model is left to a subsequent paper.

MODEL 1 — IMPLICIT PRODUCTION TECHNIQUE

Model 1 is the basic IMPES analysis[2,3] applied to the difference equations describing two- or three-phase flow in a cylindrical (r-z) geometry. In this technique the terms involving saturation changes over a given time step are eliminated by combining the original difference equations. From this result, together with the definition of capillary pressure, a single equation in either the oil or

water potential is found. The equation is solved for updated potentials over the difference grid by iterative ADI,[4] Successive Overrelaxation (SOR),[5] or directly by Gaussian elimination. The saturation-dependent terms (transmissibilities and capillary pressure) which remain in the potential equation as coefficients or constants are treated explicitly. The fact that the capillary pressure is treated explicitly in the potential equation is sufficient to cause conditional stability (i.e., a time-step restriction). After the potential distribution has been computed from the potential equation, the saturations are updated directly from the original difference equations. In this calculation the individual oil or water production rates are saturation dependent and are treated implicitly as $q_{w_n} + q'_w \Delta_t s$, where q'_w is the change in water flow rate with saturation change. The implicit production term does not complicate the direct calculation of the new saturation values since it only involves the saturation in the grid block in question. Spivak and Coats[6] found that a three- to fivefold reduction in computing time (increase in tolerable time step) followed simply from treating this production term implicitly rather than explicitly.

MODEL 2 — IMPLICIT PRODUCTION AND TRANSMISSIBILITY TECHNIQUE

The use of the implicit production term in Model 1 suggests a similar step with regard to the transmissibility terms. To preserve the simplicity of the IMPES technique, the transmissibilities still must be treated explicitly in the potential solution portion of the model. However, the saturation distribution is calculated using implicit transmissibilities. Since the transmissibilities are interblock, saturation-dependent properties, their values depend not only on the fluid saturation in the block in question, but also on the fluid saturations in the adjacent blocks. Substituting the implicit transmissibility expression (shown in detail in a later section) into the saturation equation results in a system of equations which may again be solved by ADI, SOR, or Gaussian elimination techniques. A significant feature of this model is the fact that only in the near-well region of the grid is the implicit treatment of the transmissibilities necessary so that the explicit calculation of saturation changes can be used elsewhere in the grid system. As will be shown by example, this feature allows a several-fold increase in the allowable stable time-step size while increasing the machine cost per time step by a factor less than 10 percent over Model 1. In this work, we have used ADI for solution of the potential equation (except in one application where Gaussian elimination was used) and Gaussian elimination for the implicit transmissibility region calculation. Again as in Model 1, the explicit treatment of the capillary pressure in the potential equation is sufficient to limit the size of the maximum stable time step.

TABLE 1 — MODEL COMPARISONS

Model	1	2	3
Machine time */ADI iteration/grid block	0.19	0.206	0.68
Throughput ratio — water-oil problem	19	300	15,000
Maximum time step, days — water-oil problem**	0.125	2	25
Throughput ratio — three-phase problem	—	2,250	—
Index of programming labor	1	2	6

*Univac 1108 millisec.
**Block-center radius of first block = 2.5 ft.

MODEL 3 — FULLY IMPLICIT TECHNIQUE

Model 3 differs considerably from the two models just described. The transmissibilities, potentials and capillary pressure are all taken implicitly, except for certain nonlinear terms which are dropped. Further explanation of these terms is given in the brief mathematical description found later in this paper. The implicit-difference equations written for each phase are solved simultaneously using ADI for updated potential and saturation distributions.

COMPARISON OF THE THREE MODELS

A commonly used measure of a coning model's efficiency or capability is the maximum tolerable throughput ratio R, defined as the ratio of the total fluid production rate, RB/D, from a producing grid block, multiplied by the time step, to the pore volume of the block, RB. For the water-oil coning problem described below, this ratio was 17, 300 and 15,000 for Models 1, 2 and 3, respectively. On one other water-oil coning problem studied, the fully implicit Model 3 achieved a throughput ratio R in excess of 100,000 using 90-day time steps and an 0.8 ft-block center radius at the well. These ratios along with other comparative information are given in Table 1.

Maximum tolerable time steps on a mix of gas-oil and water-oil problems were roughly in the ratio of 1:10:100. The ratio of 1:10 for Models 1 and 2 varied little over a variety of problems. The ratio of 10:100 for Models 2 and 3 varied considerably, depending upon the level of capillary pressure and the radius of the first block at the well. The reason for this is that Model 2 is conditionally stable due in large part to the explicit treatment of capillary pressure. The maximum permissible time step is inversely proportional to dP_c/dS and inversely proportional to the ratio of x-direction and z-direction transmissibilities. A small first-block radius (1 ft) gives large x-direction and small z-direction transmissibilities at the well, and Model 2 becomes highly unstable if a high-slope P_c curve is used in conjunction with a small first-block radius. In such cases the maximum time step for Model 3 can become 30 or more times larger than that for Model 2.

As given in Table 1, the computing times per grid block per (ADI) iteration are 0.19, 0.206 and 0.68 Univac 1108 millisec for Models 1, 2 and 3, respectively. The CDC 6600 is 2.2 times faster than the 1108 for these models so that corresponding

times are 0.086, 0.094 and 0.31 millisec per grid block per iteration on the CDC 6600.

Model 1 is quite easily programmed and is fast computationally. The implicit handling of the production terms in this model increases the tolerable time step by a factor of 3 to 5 over the same model with explicit production terms, while causing no increase in computing time per time step.[6] Model 2 requires more programming labor than Model 1 in respect to solution of the saturation equation. Model 3 requires considerably more programming labor than Model 2. Rough estimates of total programming and debugging time (Model 1 normalized at unity) are given in Table 1 as 1, 2 and 6 for Models 1, 2 and 3, respectively.

EXAMPLE CONING STUDIES

PROBLEM 1 — WATER-OIL MODELS 1, 2 AND 3

Blair and Weinaug have presented a coning study of an oil-water system using their fully implicit numerical model. In this study, they show a significant improvement in the maximum stable time-step size over the numerical models previously available. A study was made of their coning problem using the three models discussed here, and the computational results using the various techniques were compared.

The water-oil coning data are given in Table 2. The system being considered is a cylinder having a radius of 1,460 ft and a thickness of 360 ft, of which the top 160 ft contain oil and connate water. The vertical permeability is 1 darcy, as is the radial permeability in the oil zone. The radial permeability in the water zone is 5 darcies. The system is produced by bottom-water through a production interval extending between 80 and 100 ft below the top of the oil pay. These data are similar to that of the Blair and Weinaug study except the producing interval was lowered to 60 ft above the oil-water contact so that water breakthrough would occur sooner. Blair and Weinaug reported a stable solution using time steps of 0.2 day and using a producing block pore volume of about 4 RB. The flow per time step from the lower production block was 60 times the pore volume of that block.

Using Model 2 and a producing block pore volume (lower block) of 8 RB, the maximum time-increment size after coning phase breakthrough was found to be as high as 2.0 days, or a throughput of 310 PV at the lower grid block. Model 1 was run using the 2.0-day time step and the calculations became unstable as shown in Fig. 2. It was necessary to reduce the time-step size to 0.125 day in order to obtain usable results. The use of the implicit transmissibility model results in a 16 to 1 reduction in the computational work over Model 1 in this particular problem.

Applying Model 3 to this problem resulted in an allowable time-step size of 25 days, very near a throughput of 5,000 PV per time step. Since Model 3 requires about three times as much machine time per increment as Model 2, a fourfold increase in computational efficiency of Model 3 over Model 2 is realized in this particular problem. A block-centered radius of 2.5 ft for the producing grid block was used in obtaining these results. The water-oil ratio behavior for 1,000 days past breakthrough is presented in Fig. 3. The effect of the wellbore-grid block size was examined for Models 2 and 3 and are summarized as follows.

TABLE 2 — WATER-OIL CONING PROBLEM DATA*

Wellbore radius	0.25 ft
Exterior radius	1,460 ft
Total thickness	360 ft
Water-oil contact from top of section	160 ft
Oil viscosity	0.34 cp
Water viscosity	0.31 cp
Oil specific weight	0.36 psi/ft
Water specific weight	0.43 psi/ft
Porosity (fractional)	0.207
Radial permeability in oil zone	1,000 md
Radial permeability in water leg	5,000 md
Vertical permeability	1,000 md

Grid system:

Block-centered radii (10 blocks) —
2.5, 4.9, 9.5, 18.6, 36.3, 70.7, 138.1, 269.4, 525.7, 1,025.9

Vertical layer thickness (16 layers) —
20, 20, 20, 20, 15, 5, 20, 20, 20, 20, 30, 30, 30, 30, 30, 30

Production:

Layer	Interval (ft)	Flow Rate (RB/D)
5	80 – 95	3,752
6	95 – 100	1,248

Saturation table:

S_w	P_c	K_{ro}	K_{rw}
0.160	1.200	0.950	0.000
0.200	0.680	0.750	0.005
0.300	0.470	0.450	0.020
0.400	0.380	0.240	0.030
0.500	0.320	0.120	0.065
0.600	0.250	0.050	0.080
0.700	0.170	0.005	0.130
0.800	0.000	0.000	0.190

*Similar to the data described by Blair and Weinaug.[1]

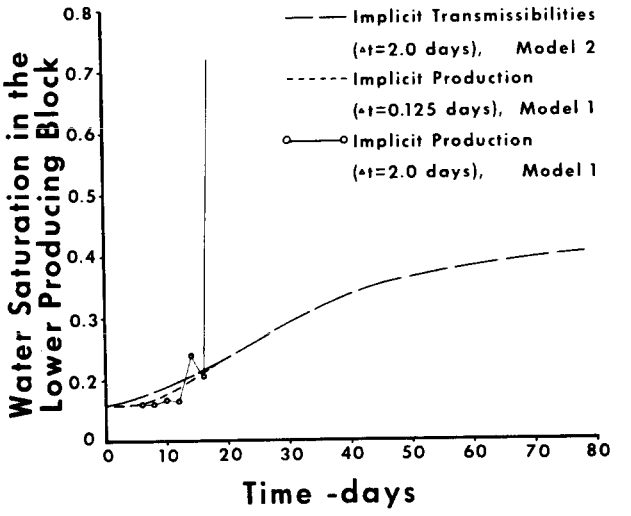

FIG. 2 — MODEL RESULTS FOR THE WATER-OIL PROBLEM.

	Wellbore Block Radius (ft)	Stable Time Step Size (days)	Throughput Per Time Step (PV)
Model 2	1.5	1.0	308
	2.5	2.0	310
	3.5	4.0	320
Model 3	2.5	25.0	5,000
	1.0	15.0	15,000

For Model 2, the maximum throughput ratio was relatively independent of the radius of the first block at the well. For Model 3, the maximum tolerable time step was relatively insensitive to the size of the first block at the well. The maximum time step fell only from 25 to 15 days as the first block-center radius decreased from 2.5 to 1.0 ft (a sixfold decrease in pore volume of the first producing block).

For each of the radii examined, the water-oil ratio vs time results obtained were the same. In general, for the limited cases studied, the results were found to be insensitive to the size of the first block-center radius if less than 5 ft.

PROBLEM 2 — THREE-PHASE, MODEL 2

Table 3 gives permeability and porosity for each of 14, 20-ft thick layers in a reservoir of exterior radius 1,560 ft. The initial gas-oil and water-oil contacts were 48 and 230 ft from the top of the sand, respectively. Water-oil and gas-oil relative permeability curves are given in Table 4. Relative permeabilities to water and gas are single-valued functions of water and gas saturations, respectively. Relative permeability to oil is $k_{rH} \times \bar{k}_{ro}$ where k_{rH} is a single-valued function of water saturation and $\bar{k}_{ro}$ is a single-valued function of total liquid saturation. Capillary pressure for this problem is zero. Formation volume factors, solution gas and viscosities are given in Table 4. Table 3 gives remaining data for the problem.

The well was completed in Layer 7 and produced a constant 400 STB/D of oil. Additional gas and water production was calculated by the model in accordance with the gas, oil and water mobilities in the producing grid block. This problem was run using Model 2 using the following time step schedule.

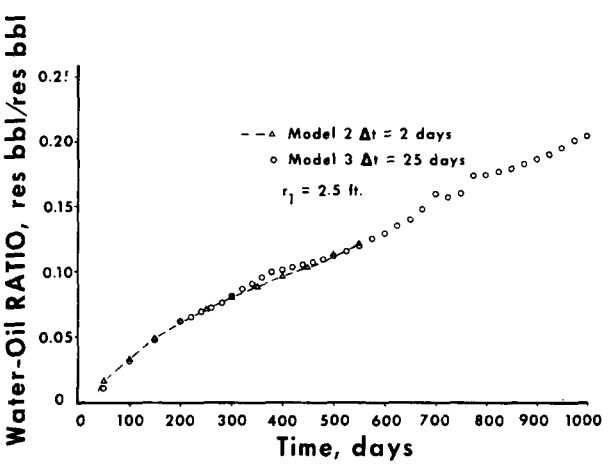

FIG. 3 — WATER-OIL CONING PROBLEM.

Time (days)	Time Step (days)
0 – 20	5
20 – 60	10
60 – 180	20
180 – 2,160	30

The run took a 60-day time step perfectly smoothly, but time truncation error became appreciable between 30- and 60-day time steps.

The average pressure in the system fell from 2,018 psi to 1,746 psi during the 6 years of production. Gaussian elimination was used to solve both the potential equation and the saturation equation over the entire grid. Fig. 4 shows the computed GOR as a function of time. Water breakthrough, defined as 0.1 BWPD water production rate, did not occur until 1,770 days, and water ptoduction rate was only 0.08 BWPD at 2,160 days.

Computing time for this 6-year (2.60-day) run was 35 seconds on the Univac 1108. This time corresponds to 0.44 seconds per time step or 4.6 microsec per time step per grid block. The throughput ratio was 2,250 for the 30-day time step.

PROBLEM 3 — LABORATORY MODEL DATA
MODEL 2

Soengkowo[7] has studied the phenomenon of water coning by means of a physical model. His model consisted of a 10° wedge out of a cylindrical section having a radius of 19.3 in. and a thickness of approximately 16 in. The oil-zone equivalent was

TABLE 3 — THREE-PHASE CONING PROBLEM DATA

Wellbore radius, ft	0.5
Exterior radius, ft	1,560
Water density, lb/cu ft stock tank	71
Oil density, lb/cu ft stock tank	51.5
Gas density, lb/Mcf	63.0
Water viscosity, cp	0.8
Water-oil contact from top of pay, ft	230
Gas-oil contact from top of pay, ft	48
Water compressibility, psi^{-1}	0.0000035
Rock compressibility, psi^{-1}	0.000004

In the reservoir:

$B_w = 1/(1 + c_w p_w)$ RB/STB

$\rho_w = 7/(1 + c_w p_w)$ lb/cu ft

$\rho_o = (51.5 + 63.0\ R_s/5.6146)/B_o$ lb/cu ft

$\rho_g = 63.0/(5.6146\ B_g)$ lb/cu ft

Block-center radii — 2.0, 5.5, 15.3, 42.4, 117.3, 324.7, 898.5

Grid layers (14):

Horizontal Permeability (md)	Vertical Permeability (md)	Porosity	Thickness (ft)
11.2000	4.3000	0.0700	20.0000
2.1000	0.6800	0.0350	20.0000
71.5000	32.2000	0.1230	20.0000
22.0000	8.0000	0.0900	20.0000
9.0000	5.5000	0.0630	20.0000
176.1000	53.0000	0.1370	20.0000
47.5000	13.6000	0.1100	20.0000
32.7000	18.4000	0.1050	20.0000
14.3000	3.2600	0.0910	20.0000
78.7000	24.1000	0.1280	20.0000
27.3000	7.1000	0.0860	20.0000
312.4000	96.2000	0.1490	20.0000
150.0000	30.0000	0.1500	20.0000
150.0000	30.0000	0.1500	20.0000

3 in. thick and made of sand consolidated with epoxy resin. A permeability of 12.1 darcies and a porosity of 30.5 percent was estimated for this sand pack. The aquifer portion of the model occupied the remaining thickness of 13 in. and was made of an unconsolidated sand. Two different aquifer sands were used during the study, having permeabilities of 15.4 and 26.5 darcies. The oil and water phases were simulated by water-base fluids which were miscible in all proportions. The fluid viscosities were controlled by the addition of glycerol and the densities by the addition of potassium iodide. The mobility ratio across the original oil-water contact was calculated as the ratio of the permeabilities in the aquifer and the oil zone, while the mobility ratio across the moving cone boundary was the ratio of viscosities between the two fluid analogs. For convenience, the model was inverted with the oil zone at the bottom and the aquifer on top. The water analog was injected at the top of the model near the outer periphery. A production port was located at the well in the bottom of the oil zone.

The data obtained from this model were presented graphically as pore volumes oil produced vs the pore volumes of water injected, where a pore volume was defined as the void volume associated with a cylinder that had both its height and radius equal to the thickness of the oil zone. Also included in these graphs were the fractional oil cut vs the pore volumes injected.

Two of Soengkowo's experimental runs were selected and his results simulated by the Model 2. These runs are referred to as 2A and 3, consistent with the original reference. Table 5 summarizes the input data for each simulation run. The relative permeability data were assumed to be linear functions of water saturation with a connate water saturation of zero and a residual oil saturation of zero. Figs. 5 and 6 show the experimental and simulator results for Runs 2A and 3, respectively. The throughput volumes and time increment sizes given in Table 5 are not necessarily the maximum values which could have been employed. The comparison between the laboratory results and the mathematical simulation is quite good and well within the range of the uncertainty in the basic input data.

TABLE 4 — PRESSURE AND SATURATION DATA FOR THREE-PHASE CONING PROBLEM

Pressure Data:

Pressure (psia)	B_o, RB/STB	B_g, RB/Mcf	R_s, Mcf/STB	V_o, (cp)	V_g, (cp)
200.0	1.14270	14.58000	0.12500	0.8900	0.0112
500.0	1.17600	5.99000	0.19000	0.7200	0.0121
700.0	1.19500	4.19000	0.23100	0.6500	0.0124
1,000.0	1.22250	2.88000	0.29100	0.5600	0.0126
1,500.0	1.26500	1.86000	0.39000	0.4700	0.0131
2,020.0	1.30770	1.36000	0.49000	0.4000	0.0143
2,500.0	1.30250	1.04000	0.49000	0.4300	0.0153
2,800.0	1.29750	0.92000	0.49000	0.4400	0.0160

Water Saturation Table:

S_w	k_{rw}	k_{rh}
0.20000	0.00000	1.00000
0.20500	0.00000	0.95000
0.22000	0.00900	0.80000
0.25000	0.02800	0.40000
0.30000	0.06000	0.16000
0.35000	0.09600	0.06600
0.40000	0.13500	0.02700
0.45000	0.17700	0.01100
0.50000	0.22200	0.00440
0.55000	0.26800	0.00180
0.60000	0.31500	0.00072
0.65000	0.36500	0.00028
0.70000	0.41700	0.00000
1.00000	0.72900	0.00000

Gas Saturation Table:

$S_o + S_w$	k_{ro}	k_{rg}
0.37500	0.00000	0.79000
0.43750	0.00140	0.70200
0.50000	0.00290	0.61500
0.56250	0.00600	0.53100
0.62500	0.01200	0.44400
0.68750	0.02600	0.35800
0.75000	0.05400	0.27800
0.81250	0.11000	0.20200
0.87500	0.23000	0.12800
0.93750	0.49000	0.06100
1.00000	1.00000	0.00000

TABLE 5 — PHYSICAL MODEL DATA[10]

	Run 2A	Run 3
Wellbore radius, in.	0.012	0.012
Exterior radius, in.	19.3	19.3
Total thickness of model, in.	16.0	16.0
Pay thickness, in.	3.0	3.0
Water-oil contact, from top of section, in.	3.0	3.0
Oil viscosity, cp	0.911	0.911
Water viscosity, cp	0.936	0.936
Oil specific weight, psi/ft	0.433	0.433
Water specific weight, psi/ft	0.510	0.510
Porosity, fractional	0.305	0.305
Pay zone permeability, darcies	12.0	12.0
Aquifer permeability, darcies	26.2	15.4
Producing interval, in.	0 – 0.75	0 – 0.75
Production rate, cu ft/D	0.814	15.77

Grid system:
Block-centered radii (9 blocks) —
0.5, 1.0, 2.0, 4.25, 6.25, 8.25, 11.0, 14.25, 17.25 (in.)
Vertical layer (5 layers) thicknesses —
0.75, 0.75, 0.75, 0.75, 16.0 (in.)

DESCRIPTION OF MODELS 1 AND 2

The mathematical descriptions presented here

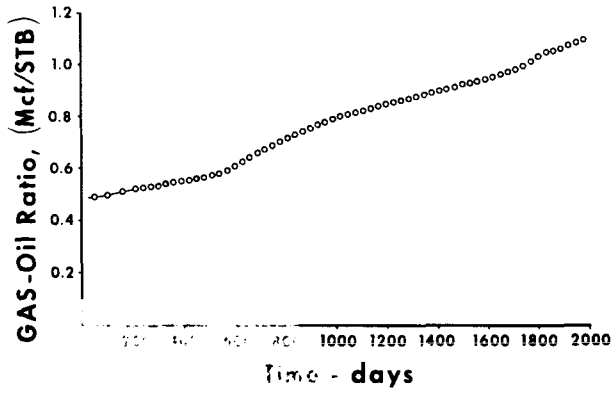

FIG. 4 — [illegible]PHASE [illegible]NG PROBLEM (COMPUTED [illegible]RY, MODEL 2).

pertain to incompressible two-phase flow of oil (o) and water (w). These stipulations are made only for clarity and do not affect the generality of the techniques presented.

The partial differential equations describing radial two-phase incompressible fluid flow in a cylindrical section are

$$\frac{1}{r}\frac{\partial}{\partial r}\left(r\frac{k_{ro}k_h}{\mu_o}\frac{\partial\Phi_o}{\partial r}\right)+\frac{\partial}{\partial z}\left(\frac{k_{ro}k_z}{\mu_o}\frac{\partial\Phi_o}{\partial z}\right) - B_o q_{vo} = \phi\frac{\partial S_o}{\partial t} \quad \ldots\ldots\ldots \text{(1a)}$$

$$\frac{1}{r}\frac{\partial}{\partial r}\left(r\frac{k_{rw}k_h}{\mu_w}\frac{\partial\Phi_w}{\partial r}\right)+\frac{\partial}{\partial z}\left(\frac{k_{rw}k_z}{\mu_w}\cdot\frac{\partial\Phi_w}{\partial z}\right) - B_w q_{vw} = \phi\frac{\partial S_w}{\partial t} \quad \ldots \text{(1b)}$$

The potentials are defined as

$$\Phi_o \equiv p_o - \gamma_o z \quad \ldots\ldots\ldots\ldots \text{(2a)}$$

$$\Phi_w \equiv p_w - \gamma_w z \quad \ldots\ldots\ldots\ldots \text{(2b)}$$

In addition, the pressures in each fluid phase can be related by capillary pressure,

$$P_c = p_o - p_w \quad \ldots\ldots\ldots\ldots \text{(3)}$$

which is taken to be a function of water saturation alone. Also, we include the obvious relation that the saturations of each phase sum to unity.

$$S_w + S_o = 1.0 \quad \ldots\ldots\ldots\ldots \text{(4)}$$

Eqs. 1a and 1b may be expressed in finite-difference form as

$$\Delta(T_o\Delta\Phi_o)_{i,j} - q_{o_{i,j}} = \frac{V_{p_{i,j}}}{\Delta t}(S_{o_{n+1}} - S_{o_n})_{i,j} \quad \ldots \text{(5a)}$$

and

$$\Delta(T_w\Delta\Phi_w)_{i,j} - q_{w_{i,j}} = \frac{V_{p_{i,j}}}{\Delta t}(S_{w_{n+1}} - S_{w_n})_{i,j} \quad \ldots \text{(5b)}$$

where

$$\Delta(T_o\Delta\Phi_o) = \Delta_r(T_{ro}\Delta_r\Phi_o) + \Delta_z(T_{zo}\Delta_z\Phi_o) \quad \ldots \text{(6)}$$

and

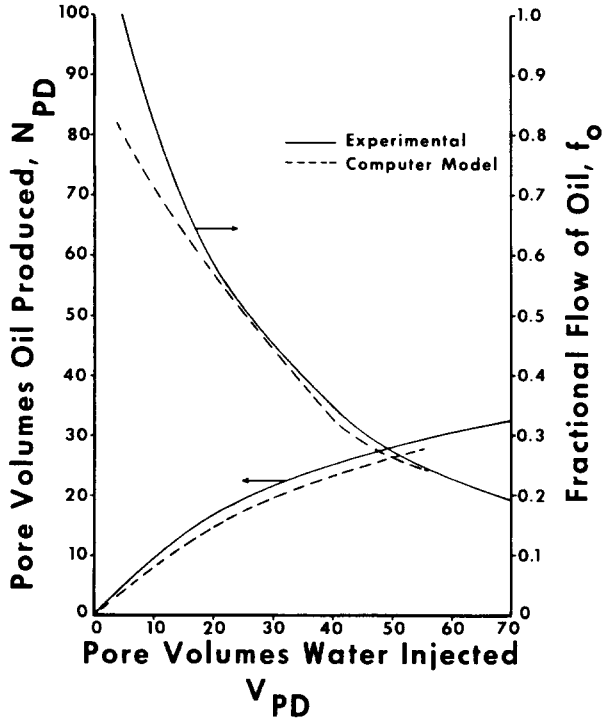

FIG. 5 — COMPARISON OF PHYSICAL MODEL[7] AND NUMERICAL MODEL RESULTS, RUN 2A.

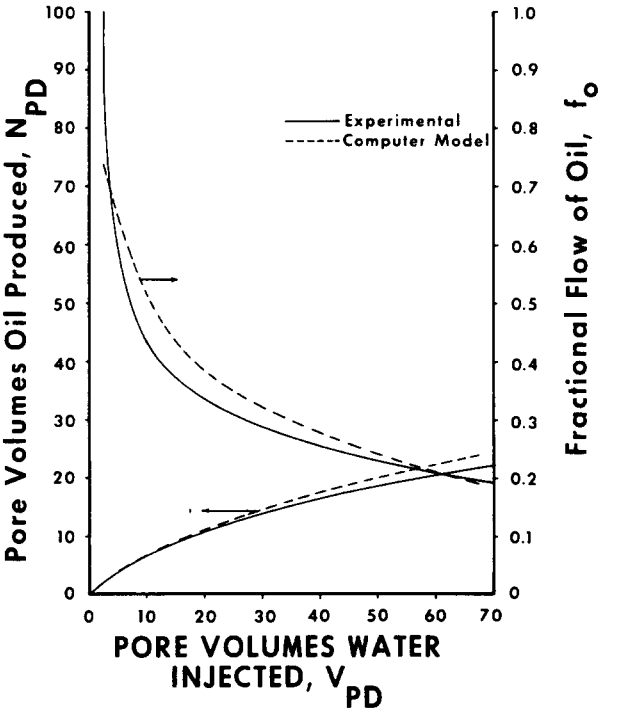

FIG. 6 — COMPARISON OF PHYSICAL MODEL[7] AND NUMERICAL MODEL RESULTS, RUN 3.

$$q_{o_{i,j}} = B_o q_{vo} V_{b_{i,j}} \text{ cu ft/D} \quad \ldots\ldots (7)$$

The coefficients of the pressure differences are defined as transmissibilities. In the radial direction,

$$T_{ro_{i-\frac{1}{2},j}} \equiv \frac{2\pi(\Delta z)_j (k_h k_{ro})_{i-\frac{1}{2},j}}{\mu_o \ln(r_i/r_{i-1})} \quad (8)$$

and for the vertical direction,

$$T_{zo_{i,j-\frac{1}{2}}} \equiv \frac{2\pi(r^2_{i+\frac{1}{2}} - r^2_{i-\frac{1}{2}})_i (k_z k_{ro})_{i,j-\frac{1}{2}}}{\mu_o \left[(\Delta z)_j + (\Delta z)_{j-1}\right]} \quad (9)$$

where the units of T_{ro} and T_{zo} are cubic feet of fluid per day per psi potential drop. The block-centered radii, r_i, $i = 1, I$, illustrated in Fig. 7, can be specified arbitrarily but are generally spaced geometrically,

$$r_i = \alpha^{i-1} r_1 \quad \ldots\ldots (10)$$

where α is a constant chosen so that

$$r_e = (r_{I+1} - r_I) / \ln \frac{r_{I+1}}{r_I} \quad \ldots (11)$$

That is, α is chosen so that the exterior radius is the log-mean radius between r_I and r_{I+1}. The block boundary radii, $r_{i+\frac{1}{2}}$, are the log-mean radii

$$r_{i+\frac{1}{2}} = \frac{r_{i+1} - r_i}{\ln \frac{r_{i+1}}{r_i}} \quad \ldots\ldots (12)$$

MODEL 1

The IMPES method[2,3] is probably the most direct technique for solving the simultaneous two-phase fluid flow equations. The first step in applying this technique is the elimination of the saturation variable. When Eqs. 5 are added together, the sum of the terms on the right-hand side of the equation is zero since the total saturation ($S_o + S_w$) must always be unity. The result is an equation of elliptic type in the oil and water potentials.

$$\Delta(T_o \Delta\Phi_o)_{i,j} + \Delta(T_w \Delta\Phi_w)_{i,j} - (q_o + q_w)_{i,j} = 0 \quad \ldots\ldots (13)$$

Note that the production term is now the total fluid production rate from the grid block which shall be designated as

$$q_{i,j} \equiv q_{o_{i,j}} + q_{w_{i,j}} \quad \ldots\ldots (14)$$

This total production rate is known. The relative amounts of oil and water production must be computed from the saturation-dependent mobilities of the two fluids in the production grid block. Using the definitions of potential and capillary pressure (viz., Eqs. 2 and 3, respectively), Eq. 13 may be written in terms of a single potential in the form,

$$\Delta(T\Delta\Phi_w)_{i,j} = B_{i,j} \quad \ldots\ldots (15)$$

where $T = T_o + T_w$. This equation may be solved by ADI, SOR, or Gaussian elimination for the potential distribution. All saturation-dependent terms (i.e., transmissibilities and capillary pressure) are taken at the previous time level n.

The saturation may be computed directly from Eqs. 5. However, we must first determine the implicit production term. The oil-flow rate from a particular grid block can be expressed in terms of the fractional flow of water by

$$q_{w_{i,j}} = f_{w_{i,j}} q_{i,j} \quad \ldots\ldots (16)$$

The fractional flow of water is defined in terms of the viscosities and relative permeabilities as

$$f_w = \frac{k_{rw}/\mu_w}{(k_{rw}/\mu_w) + (k_{ro}/\mu_o)} \quad (17)$$

The term f_{w_n} is known as a function of the old value of water saturation. The n+1 time-level value of f_w can be estimated from a truncated Taylor's series expansion about (f_{w_n}, S_{w_n})

$$f_{w_{n+1}} = f_{w_n} + f'(S_{w_{n+1}} - S_{w_n}) \quad (18)$$

where the chord slope approximation to derivative df/dS is used to define f'

$$f' = \frac{(f_{w_{n+1}} - f_{w_n})}{(S_{w_{n+1}} - S_{w_n})} \quad \ldots\ldots (19)$$

There are two alternative means of computing the chord slope (f') in Eq. 19. Either an iterative procedure converging to f_{n+1} may be used or, more

simply, f' may be estimated from the f vs S_w relation in the neighborhood of S_{w_n}. This latter course was found to be the most direct and efficient means of obtaining f'. Since the f vs S_w relation is given in tabular form, the chord slope f' is taken as the straight-line slope of the table in the interval where S_{w_n} is found.

Having an expression for the fractional flow at the n+1 level, the "implicit" water production from the grid block may be expressed as

$$q_{w_{n+1}} = q_{w_n} + q\, f'(S_{w_{n+1}} - S_{w_n}) \quad \ldots\ldots\ldots\ldots (20)$$

We now replace the n-level water production term in Eq. 5b by the "implicit" water production term expressed above and obtain

$$S_{w_{n+1}} = S_{w_n} + [\Delta(T_w \Delta\Phi_w) - q_w]_{i,j,n} \Big/ \left(\frac{V_p}{\Delta t} + q f'\right)_{i,j} \quad (21)$$

MODEL 2

The implicit production procedure applied to the wellbore production grid blocks suggests a similar step with regard to the transmissibilities in the grid blocks near the wellbore. However, additional assumptions must be considered when analyzing this possibility.

First, consider the potential Eq. 15

$$\Delta(T\Delta\Phi_w)_{i,j} = B_{i,j} \quad \ldots\ldots\ldots (15)$$

We note that the transmissibilities enter into the pressure solution, whereas in the source term only the total production rate is needed rather than the separate oil or water production rates. The transmissibilities must be treated explicitly in the potential equation to preserve the simplicity of the IMPES analysis. We will therefore neglect the effect of implicit transmissibilities on the pressure solution.

Now we may examine the saturation calculation Eq. 21 again. This time we shall expand the equation, writing the transmissibilities and oil production rates in terms of the n+1 time level.

$$\Delta(T_{w_{n+1}} \Delta\Phi_{w_n})_{i,j} - q_{w_{i,j,n+1}} = \frac{V_{p_{i,j}}}{\Delta t}(S_{w_{n+1}} - S_{w_n})_{i,j} \quad \ldots (22)$$

The method for calculating the updated water production has been described above. Updating the interblock transmissibilities is done in a similar fashion but is complicated by the fact that the saturations of two adjacent grid blocks must be considered. As with the production term, the transmissibility at the n+1 time level is given as

$$T_{w_{i,j,n+1}} = A_{w_{i,j}} [(1-w)k_{rw_{i,j,n+1}} + w k_{rw_{i-1,j,n+1}}] \quad \ldots (23)$$

where A_w contains the non-saturation dependent terms in the transmissibility definition. The values of $k_{w_{n+1}}$ can be approximated by

$$k_{rw_{n+1}} = k_{rw_n} + k'(S_{w_{n+1}} - S_{w_n}) \quad \ldots\ldots\ldots\ldots\ldots (24)$$

which is similar to the expression for fractional flow, Eq. 18, and where k' is the chord slope of the k_{rw} vs S_w relationship.

$$k' \equiv \frac{k_{rw_{n+1}} - k_{rw_n}}{S_{w_{n+1}} - S_{w_n}} \quad \ldots\ldots (25)$$

Combining Eqs. 24 and 25

$$T_{w_{i,j,n+1}} = T_{w_{i,j,n}} + A_{w_{i,j}} [(1-w)k'_{i,j}(\Delta_t S)_{i,j} + w k'_{i-1,j}(\Delta_t S)_{i-1,j}] \quad \ldots\ldots (26)$$

where

$$\Delta_t S = S_{w_{n+1}} - S_{w_n} \quad \ldots\ldots (27)$$

The weighting factor w is taken as 0 or 1 to weight relative permeability upstream. We have found a direct estimate of the chord slope k' in the neighborhood of S_{w_n} to be sufficient. That is, neither the computed results nor maximum time step are affected by rigorously calculating k' as in Eq. 25 as opposed to using the slope obtained from the relative permeability table at S_{w_n}.

Substituting Eqs. 20 and 26 into Eq. 22 gives, after considerable algebraic bookkeeping, an expression of the form

$$C_{i+1,j}(\Delta_t S)_{i+1,j} - D_{i,j}(\Delta_t S)_{i-1,j} + E_{i,j+1}(\Delta_t S)_{i,j+1} - F_{i,j}(\Delta_t S)_{i,j-1} + G_{i,j}(\Delta_t S)_{i,j} = H_{i,j} \quad \ldots\ldots (28)$$

where C, D, etc., are expressions involving transmissibility-pressure difference terms. The number of grid blocks in which the transmissibilities are treated implicitly may be limited to those near the wellbore. The matrix which results when Eq. 28 is written for the grid blocks desired is well-conditioned and is readily solved by the Gaussian elimination technique. In Model 2 Eq. 28 is used to find the new saturations in the designated implicit transmissibility region, and Eq. 21 is employed over the rest of the grid.

BRIEF DESCRIPTION OF MODEL 3

Finite-difference Model 3 differs considerably from the two models just described. Eqs. 5a and 5b are written implicitly as

$$[\Delta T_w \Delta \Phi_w]_{n+1} - q_{w_n} =$$

$$[q'_w + \frac{V_p}{\Delta_t}] \Delta_t S_w [\Delta T_o \Delta \Phi_w]_{n+1}$$

$$+ [\Delta T_o \Delta (P_c + \Delta \gamma z]_{n+1} - q_{o_n} =$$

$$-[q'_w + \frac{V_p}{\Delta_t}] \Delta_t S_w, \quad \ldots\ldots\ldots (29)$$

where transmissibilities, potentials and capillary pressure are all taken implicitly. Actually, a nonlinear term is dropped as

$$[\Delta T \Delta \Phi]_{n+1} \equiv \Delta(T_n + \delta T)\Delta(\Phi_n + \delta \Phi) \cong$$

$$\Delta T_n \Delta \Phi_n + \Delta \delta T \Delta \Phi_n + \Delta T_n \Delta \delta \Phi \quad \ldots (30)$$

where δT, $\delta \Phi$ are the changes over the time step in transmissibility and potential. Eq. 29 is solved simultaneously using ADI for the two unknowns $\Phi_{w_{n+1}}$ and $S_{w_{n+1}}$ over the grid.

TRUNCATION ERRORS

Aside from stability considerations, the effect of truncation errors must also be considered when evaluating the performance of a model. In this section we will show that for the incompressible case (as is the Blair-Weinaug example coning problem) the implicit transmissibilities result in larger truncation errors than do explicit transmissibilities. The simple waterflood equation,

$$-\frac{\partial f}{\partial x} = \frac{\partial S}{\partial t}, \quad \ldots\ldots\ldots\ldots (31)$$

will be used to illustrate this point. The explicit difference approximation to Eq. 31 is written

$$\frac{f_{i,n} - f_{i-1,n}}{\Delta x} = \frac{S_{i,n+1} - S_{i,n}}{\Delta t} \quad \ldots (32)$$

With suitable definitions of x and t, this equation is exactly equivalent to Eqs. 5a and 5b for the case where (a) flow is one-dimensional, (b) capillary pressure is neglected, (c) explicit transmissibilities are used in Eqs. 5a and 5b, (d) injection-production occurs at the ends of the one-dimensional system, and (e) interblock relative permeabilities in Eqs. 5a and 5b are weighted upstream.

The truncation error of Eq. 32 defined as

$$T_E \equiv \frac{f_{i,n} - f_{i-1,n}}{\Delta x} - \frac{S_{i,n+1} - S_{i,n}}{\Delta t}$$

$$- (-f_x - S_t)_{\substack{x=i\Delta x \\ t=(n+\frac{1}{2})\Delta t}} \quad \ldots (33)$$

is

$$T_E = S_{x_t}(\frac{\Delta x}{2} - \frac{\Delta t}{2} f') \quad \ldots\ldots (34)$$

where f' is df/dS. Higher order terms have been dropped in this development, as is customary in truncation error analyses.

The implicit-difference approximation to Eq. 31 is

$$\frac{f_{i,n+1} - f_{i-1,n+1}}{\Delta x} = \frac{S_{i,n+1} - S_{i,n}}{\Delta t} \quad \ldots\ldots\ldots\ldots (35)$$

This equation is exactly equivalent to Eqs. 5a and 5b for the above listed conditions, with the exception of use of implicit transmissibilities in Eqs. 5a and 5b. The truncation error of Eq. 35, defined in a fashion analogous to Eq. 33 is

$$T_I = S_{x_t}(\frac{\Delta x}{2} + \frac{\Delta t}{2} f') \quad \ldots\ldots (36)$$

Comparison of Eqs. 34 and 36 shows that the truncation error for the explicit-difference scheme is always less than the truncation error of the implicit scheme.

The explicit scheme, Eq. 32, is stable only for $\Delta t \leq \Delta x/f'$. We have numerically solved Eqs. 32 and 35 and noted the more accurate results from Eq. 32 when compared to the analytical (Buckley-Leverett) solution. We note that this lesser truncation error for the explicit-transmissibility scheme follows from an analysis of incompressible fluid flow.

COMPARISON OF ADI AND GAUSSIAN ELIMINATION

In the description of the simulation models

presented above we have referred repeatedly to the option between the use of ADI and Gaussian elimination techniques for solution of the potential and saturation equations. The computational work required for solution of the pressure Eq. 15 is expressed here in terms of the number of multiplications + divisions needed for a given grid system ($I \times J$) as shown in Fig. 7. The work per iteration associated with the ADI technique is $13IJ$. Gaussian elimination for the symmetric matrix represented by Eq. 15 requires work of $I^3J/2$ assuming $I < J$ and a linear numbering of grid points in the radial direction as shown by the numbers in parentheses on Fig. 7.

Denoting the number of ADI iterations necessary to reach convergence by K, we find that Gaussian elimination requires less work and computing time than ADI when

$$I^3J/2 < 13\,IJK \quad \ldots\ldots\ldots\ldots (37)$$

or

$$I < \sqrt{26K} \quad \ldots\ldots\ldots\ldots (38)$$

We have found a K of 16 to be typical in a variety of coning problems. Thus Gaussian elimination is preferable to ADI for an incompressible problem when $I < 20$. For the compressible case, the matrix associated with the pressure equation is not symmetric, and the work of Gaussian elimination is I^3J. Again using $K = 16$, we find Gaussian elimination is preferable to ADI provided $I < 14$.

If $J < I$, then the above results are modified in that Gaussian elimination is preferable to iterative ADI when $J < 20$ or $J < 14$.

Apart from computing work, Gaussian elimination elimination does away with the problem of selecting ADI iteration parameters. However, we have experienced very little difficulty in selecting effective ADI iteration parameters.

CONCLUSIONS

Results of our study indicate:

1. Model 2, the IMPES model with implicit transmissibilities, requires only 10 percent more computing time per time step than Model 1, the implicit production IMPES model, but allows a time step some 16 times larger for a water-oil coning problem studied.

2. The IMPES Model 2 becomes markedly less efficient than fully implicit Model 3 on problems where the producing-grid-block pore volume is small and capillary forces are high.

3. Model 3, the "fully implicit" model, requires approximately 3.3 times more computing time per increment than that required by Model 2. However, the large pore volume throughput (15,000 in Problem 1 for a 1-ft block-center radius) attainable with this model results in a substantially higher computing efficiency than that possible with Model 2.

4. On the limited number of problems studied, the results obtained appear to be insensitive to the first block-center radius when it is less than 5 ft.

5. For problems having only moderate capillary forces and not requiring fine grid spacing near the well, Model 2 compares favorably with Model 3 in computational efficiency.

6. Truncation error is larger when implicit transmissibilities are employed rather than explicit transmissibilities in the incompressible fluid case where upstream weighting of relative permeability is used.

7. Computing work required to solve the pressure equation is less for Gaussian elimination than for iterative ADI when the lesser of the numbers of grid blocks in the radial and vertical directions is less than 14.

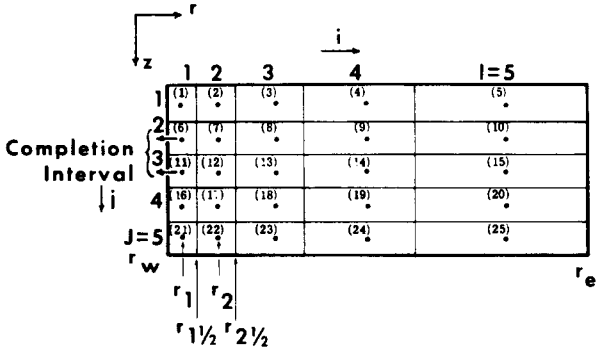

FIG. 7 — BLOCK-CENTERED COMPUTING GRID.

NOMENCLATURE

B_o = formation volume factor for oil, cu ft/STB
B_w = formation volume factor for water, cu ft/STB
f_w = fractional flow of water
I = number of grid blocks in radial direction
J = number of grid blocks in vertical direction
k_h = absolute radial (horizontal) permeability (0.00633 × md)
k_z = absolute vertical permeability (0.00633 × md)
k_{ro} = oil relative permeability
k_{rw} = water relative permeability
P_c = oil-water capillary pressure, psi
p_o = oil pressure, psia
p_w = water pressure, psia
q_{vo} = oil production, STB/cu ft reservoir-day
q_{vw} = water production, STB/cu ft reservoir-day
$q_{o_{i,j}}$ = oil production from grid block (i,j), cu ft/day
$q_{w_{i,j}}$ = water production from grid block (i,j), cu ft/day
$q_{i,j}$ = total fluid production from grid block (i,j), cu ft/day
r = radial distance, ft
$r_{i+½}$ = log-mean radius between r_{i+1} and r_i, ft
S_o = saturation of oil, fractional

S_{x_t} = $\partial^2 S/\partial x \partial t$

S_w = saturation of water, fractional

t = time, days

T = total transmissibility, $T_o + T_w$, cu ft/day – psi

T_o = oil transmissibility, cu ft/day – psi

T_{ro} = radial oil transmissibility, cu ft/day – psi

T_{zo} = vertical oil transmissibility, cu ft/day – psi

T_w = water transmissibility, cu ft/day – psi

$V_{b_{i,j}}$ = bulk volume of grid block (i,j), cu ft

$V_{p_{i,j}}$ = pore volume of grid block (i,j), cu ft

z = vertical distance measured positively downward, ft

γ_o = specific weight of oil at reservoir conditions, $\rho_o g/144 g_o$, psi/ft

γ_w = specific weight of oil at reservoir conditions, $\rho_w g/144 g_o$, psi/ft

μ_o = oil viscosity, cp

μ_w = water viscosity, cp

Φ_o = oil potential, psia

Φ_w = water potential, psia

ϕ = porosity, fractional

ACKNOWLEDGMENTS

The first author would like to express his appreciation to the Texas Petroleum Research Committee for its financial support of this study.

REFERENCES

1. Blair, P. M. and Weinaug, C. F.: "Solution of Two-Phase Flow Problems Using Implicit-Difference Equations", *Soc. Pet. Eng. J.* (1960) 417-424.
2. Stone, H. L. and Garder, A. O., Jr.: "Analysis of Gas-Cap or Dissolved-Gas Drive Reservoirs", *Soc. Pet. Eng. J.* (June, 1961) 92-104.
3. Sheldon, J. W., Harris, C. D. and Bavly, D.: "A Method for General Reservoir Behavior Simulation on Digital Computers", paper SPE 1521-G, presented at SPE 35th Annual Fall Meeting, Denver, Colo., Oct. 2-5, 1960.
4. Peaceman, D. W. and Rachford, H. H., Jr.: "The Numerical Solution of Parabolic and Elliptic Differential Equations", *J. Soc. Indust. Appl. Math.* (1955) Vol. 3, 28.
5. Young, D.: "The Numerical Solution of Elliptic and Parabolic Differential Equations", *Survey of Numerical Analysis*, J. Todd, Ed., McGraw-Hill Book Co., Inc., New York (1962) 380.
6. Spivak, A. and Coats, K. H.: "Simulation Techniques for Two- and Three-Phase Coning Studies", *Soc. Pet. Eng. J.* (Sept., 1970) 257-267.
7. Soengkowo, I.: "Model Studies of Water Coning in Petroleum Reservoirs with Natural Water Drives", PhD dissertation, The U. of Texas at Austin (May, 1969).

★★★